Experimental Results of Parallel Active Filter Implementation in Nonideal Power Grid

Oleksandr Husev, Andrei Blinov, and Dmitri Vinnikov

Tallinn University of Technology, Electrical Drives and Power Electronics,
Ehitajate tee 5,19086 Tallinn, Estonia

Abstract. This paper is devoted to the implementation of a parallel active power filter prototype in a nonideal power grid. The control algorithm is described and realized. Simulation and experimental results proved the theoretical prediction. Analytical conditions of the usable implementation are shown. Some guidelines are presented in the conclusion.

Keywords: parallel active power filter, power grid, control system, efficiency.

1 Introduction

Enhanced quality requirements for the mains current supplied by the power network require devices compensating the reactive power in both the fundamental frequency and higher harmonics. The principal advantage of active filters (AF) is in their ability to compensate a wide spectrum of higher harmonics.

The design of all active filters includes a storage element, a converter and a charger [1]-[3]. Fig. 1 represents implementation of a parallel active power filter (PAPF) in a nonideal power grid. Active filters exist in a large variety of topologies [1]-[4]. They allow compensation of a wide spectrum of the load current, although they are not free of shortcomings - namely, a limited maximum amplitude of reactive power fluctuations and the complexity of implementation.

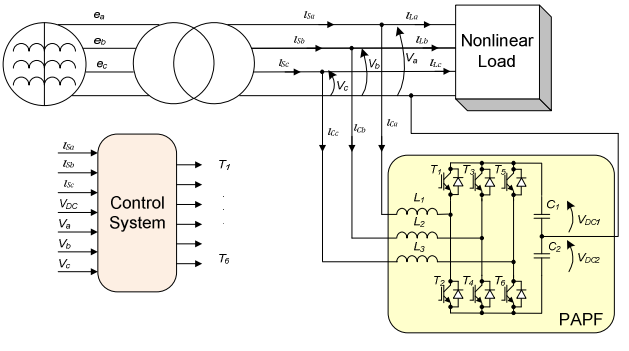

Fig. 1. A nonideal power grid with a PAPF

L.M. Camarinha-Matos et al. (Eds.): DoCEIS 2012, IFIP AICT 372, pp. 291–298, 2012.

The latter issue becomes more urgent of increasing power quality demands for power energy consumers. Energy efficiency of old power distribution and consumption systems is at least three times lower than in European requirements.

Numerous articles are devoted to the shunt active filters that contain nothing but theoretical description [5], [6]. At the same time this problem should be solved taking into account real time power grid conditions. Old power distribution equipment cannot be replaced immediately, but the efficiency should be increased.

This paper covers practical implementation of a PAPF in a nonideal power grid. The power grid in the point common connection (PCC) is represented by a three-phase power transformer with nonideal parameters. Focus is on the behavior of a PAPF in such PCCs.

Theoretical, simulation and experimental results are shown. Some guidelines are presented in the conclusion

2 Contribution to Value Creation

The value creation topic is strictly connected with power quality supplied system. The PAPF implementation poses new and interesting practical problems concerning power quality and their mutual influences. The quality of the delivered power often depends on the power load interfaces. Due to their nonlinear nature, these loads inject harmonics current into the power system and cause voltage harmonics distortion. In order to keep the quality of the power delivery system it is important to eliminate harmonics current and estimate influences of PAPF on the voltage quality. The presented work is a contribution for the power quality problem and thus for the increasing value creation of the general system

3 Control System

The control system is based on the power balance method [7]. Fig. 2 presents a block diagram of a control system for a PAPF.

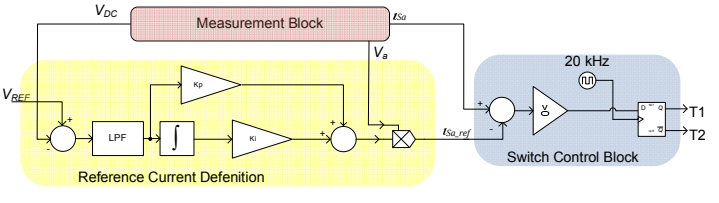

Fig. 2. Control system structure of a PAPF

The control system consists of a measurement block, a reference current definition block and a switch control block.

The main idea of the power balance method is to maintain the DC voltage level across the capacitors. The input values of the regulator enter the instantaneous value

of the voltage across the capacitors (V_{DC1}, V_{DC2}) and the reference voltage V_{REF}, equal to the necessary values of the voltage. In order to eliminate voltage pulsations across the capacitors, only the constant component of the voltage is used. Further, an error on the voltage will be given to the PI regulator whose output determines the amplitude of the reference current. The form of the reference current is determined by the supply voltage, as a result, the current is in-phase to the voltage. Further, the reference current will be given to the switch control block. The switch control block is built according to the direct current control method. Thus, transfer of the necessary active power from the grid is ensured. In the steady state mode the value of an error is equal to zero, values from the output of the integrator are constant. In this case the power consumed by the load is equal to the power that is consumed from the generator.

The main advantage of the proposed algorithm is in the reduced number of current sensors. Taking into account the EMC problem that usually is present in the real system, the reduced number of measurement values increases the stability of the control system. For example, control systems based on the PQ theory are less feasible because they demand more measurement elements

4 Simulation Results

A simplified equivalent circuit of a power grid for one phase is shown in Fig. 3*a*. The induction voltage regulator is substituted by the voltage source e_a, the internal resistances R_0 and the internal leakage inductance L_0. The transformer is substituted by the equivalent circuit with primary and secondary internal resistances R_1 and R_2, primary and secondary internal leakage inductances L_1 and L_2 and magnetizing inductance L_M. We assume that these parameters are equal in all phases.

A PARF is represented taking into account the internal inductance resistance R_a and transistor parameters. Nonlinear load is represented by a passive rectifier with a capacitor output filter that is one of the worst cases for a power grid.

Equivalent circuits for switching transistors are shown in Figs. 3*b* (T_1 is opened) and 3*c* (T_2 is opened).

From the analysis of equivalent circuits it is evident that active filter commutation disturbs the output transformer voltage shape. We can write:

$$e_S = L_{L2} \cdot \frac{di_C}{dt} + i_C(R_2 + R_a) + L \cdot \frac{di_C}{dt} \pm \frac{V_{DC}}{2}, \tag{1}$$

$$V_S = i_C \cdot R_a + L \cdot \frac{di_C}{dt} \pm \frac{V_{DC}}{2}, \tag{2}$$

$$e_S = \Delta V + V_S. \tag{3}$$

Assuming that the voltage source e_S has a pure sinusoidal shape we can express the relative voltage distortion $\frac{\Delta V}{e_S}$ by

$$\frac{\Delta V}{e_S} = \frac{L_{L2} \cdot \frac{di_C}{dt} + i_C \cdot R_2}{L_{L2} \cdot \frac{di_C}{dt} + i_C(R_2 + R_a) + L \cdot \frac{di_C}{dt} \pm \frac{V_{DC}}{2}}. \tag{4}$$

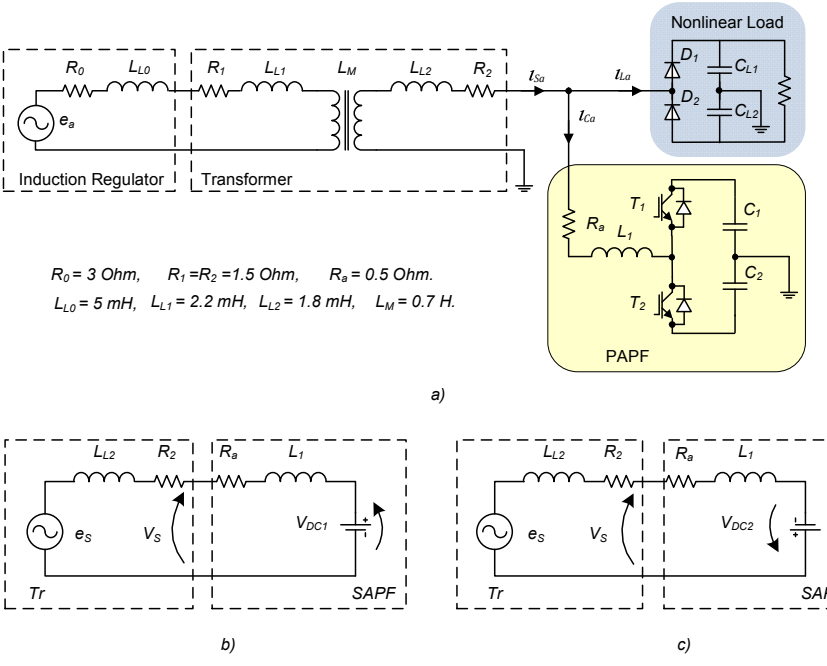

Fig. 3. Equivalent circuits of a nonideal power grid

As it can be seen from Eq. (4), relative voltage distortion depends on the DC capacitor voltage and the ratio between the leakage inductance of the transformer and the inductance of the compensator. The lower the leakage inductance the lower the distortion is.

In order to verify the presented control algorithm and the analytical prediction the MATLAB simulations were performed.

The passive components of the compensator and the minimum frequency of the commutation of power switches with the direct control method were calculated according to [8]:

$$C = \frac{4 \cdot \gamma \cdot Q_m}{K \cdot V_{DC1} \cdot \omega \cdot V_m} = \frac{4 \cdot \frac{1}{6} \cdot 380}{0.1 \cdot 125 \cdot 2\pi \cdot 50 \cdot 98} = 0.6\ mF, \tag{5}$$

$$L = \frac{V_{DC1} - V_m}{I'_{cm}} = \frac{125 - 98}{1.2 \cdot 10^4} = 2.2\ mH, \tag{6}$$

where:

Q_m – amplitude of the pulsation of the reactive power in the three-phase network;
γ – the relative duration of the pulsation of the reactive power;
ω – network frequency;
V_m – amplitude value of the phase voltage;
V_{DC} – value of voltage on the capacitor;
K – ripple factor of voltage on the capacity;
I'_{cm} – maximum value of the rate of current changing.

It should be noted that an additional RLC passive filter was used in the measurement system to obtain the reference voltage shape.

The first simulation diagrams shown in Fig. 4 correspond to the idle power grid mode (Fig. 4*a*) and the nominal power mode without a PAPF (Fig. 4*b*).

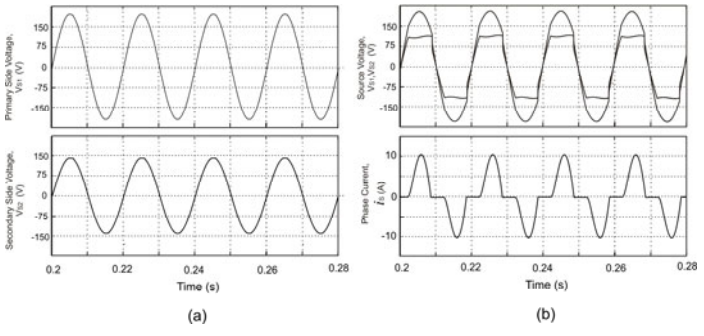

Fig. 4. Simulation diagrams without a PAPF

During the idle mode, primary and secondary voltage shapes are purely sinusoidal. After the load connection, voltage shapes are greatly disturbed. It shows the influence of the nonlinear load on the power quality in the power grid with nonideal parameters. The total consumed power is P_1 = 1300 W, on the secondary side is P_2 = 1050 W. As a result, the efficiency of the chosen transformer is about 80%. Voltage and current THD on the secondary side are about 19.5% and 47.3%, correspondingly.

The second simulation diagrams in Fig. 5 shows power grid conditions with a PAPF.

The reference phase voltage is shown in Fig. 5*a*. The compensator current is represented in Fig. 5*b*. The primary and secondary power grid currents are shown in Fig. 5*e*. The reference voltage and source current THD on the secondary side are about 28.4% and 18.7%, respectively. We can see that after the inclusion of the PAPF, the current shape is improved but the voltage shape is impaired. It is proved by the secondary and primary winding voltage (Figs. 5*b* and 5*d*).

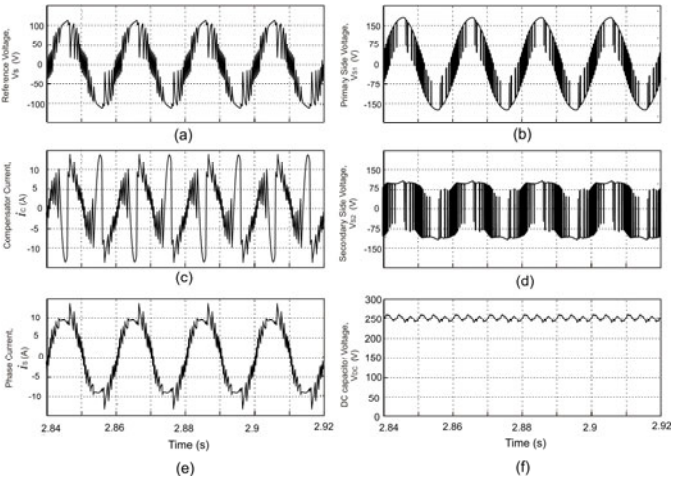

Fig. 5. Simulation diagrams with a PAPF

The DC link voltage is shown in Fig. 5*f* that proves the steady state mode.

The total consuming power on the primary side is increased to P_1 = 1950 W, on the secondary side to P_2 = 1450 W. The output consuming power is about 1340 W. As a result, PAPF efficiency is about 92%. It should be noted that modeling losses parameters of a PAPF correspond to the worst real IGBT transistors that can be used in such systems. The frequency of commutation is 10 kHz.

Simulation parameters and results are summarized and shown in Table 1.

Table 1. Simulation parameters and results

Power Grid Parameters	PAPF Parameters	RLC Filter Parameters	Simulation Results	
			Without PAPF	With PAPF
$\omega = 2\pi \cdot 50\,Hz$ V_{S1} = 133 V L_{L0} = 5 mH L_{L1} = 2.2 mH L_{L2} = 1.8 mH R_0 = 3 Ohm $R_1 = R_2$ = 1.5 Ohm	$V_{DC} = V_{DC1}+V_{DC2}$ = 250 V L = 2.2 mH $C_1 = C_2$=0.56 mF R_A = 0.5 Ohm F=10 kHz	R_F = 300 Ohm L_F = 0.5 mH C_F=1 μF	P_1 = 1300 W P_2 = 1050 W P_{OUT} = 1050 W THD_{U2} = 19.5% THD_{I2} = 47.3%	P_1 = 1950 W P_2 = 1450 W P_{OUT} = 1336 W THD_{U2} = 28.4 % THD_{I2} = 18.7%

5 Experimental Results

A laboratory prototype is shown in Fig. 6. It consists of a transformer (Fig. 6*b*), a nonlinear load (three-phase rectifier, capacitor, resistor) and a PAPF.

The PAPF is separately shown in Fig. 6*a* and consists of an inverter, optically isolated drivers for IGBTs, inductors, capacitors, measurement and control systems.

An inverter is built on BSM75GB120DLC 1200V/75A IGBT transistors. Hall effect current sensors and optically isolated voltage sensors represent the measurement system. The digital control system is based on the digital signal processor TMS320F28335.

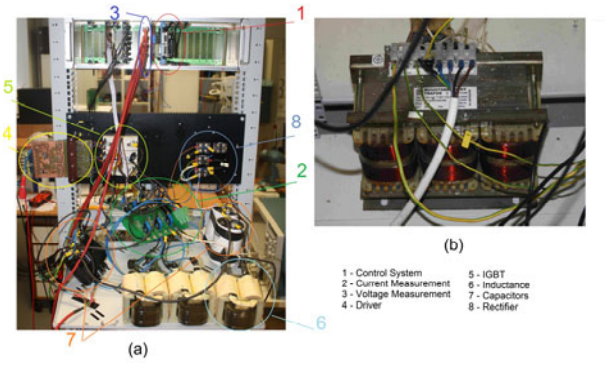

Fig. 6. Laboratory prototype of a PAPF

An induction regulator is used as a primary voltage generator. A serial buck transformer was used like a secondary voltage source. Leakage inductance and internal resistance of the secondary winding are 1.8 mH and 1.5 Ohms, respectively. The nominal transformer power is 2.5 kW, turns ratio 1.35.

Experiments with the PAPF were performed according to the simulation parameters (Fig. 7). Control was realized by the direct current control method at 10 kHz switching frequency.

It is evident that the voltage and the current are not of purely sinusoidal shape. It is explained by nonideal power grid parameters.

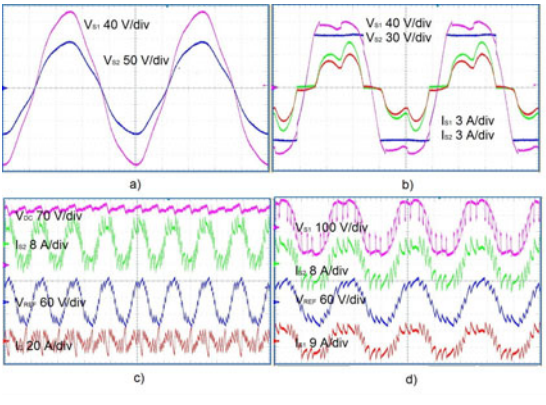

Fig. 7. Experimental results of a PAPF

The consuming primary power without a PAPF was equal to P_1=3·115 V·3.9 A=1345 W. The consuming power in the load was P_{OUT} = 1010 W. Transformer efficiency was about 75 %. In the steady state mode with a PAPF the rms phase voltage V_{S2} and current I_{S2} were equal to 83 V and 5.3 A, respectively. The output DC voltage V_{OUT} was equal to 195 V and the load current I_{OUT} to 6.1 A. As a result, the output consuming power increased to P_{OUT} = 1190 W. Taking into account

the total input consuming power P_1 = 1720 W and the secondary winding consuming power P_2 = 3·83·5.2=1295 W, it can be concluded that transformer efficiency was about 75 %. The PAPF efficiency was about 91 % that is close to the simulation results.

6 Conclusions

This paper presents a PAPF implementation prototype in a nonideal power grid. The power balance based control algorithm is described and realized. Voltage distortion as the main problem in similar power grids was analytically estimated. Simulation and experimental results proved the theoretical prediction. Analytical conditions of the usable implementation were presented. A PAPF cannot be an effective solution in power grids where leakage inductance is close to the active filter inductance. In such systems a PAPF improved current quality and total power quality slightly. Total consuming power had increased (up to 30 %), the reactive power did not decrease significantly. At the same time voltage THD level increased. In order to improve voltage quality an additional serial active power filter is required

Acknowledgement. This research work has been supported by Estonian Ministry of Education and Research (Project SF0140016s11), Estonian Science Foundation (Grant ETF8538) and Estonian Archimedes Foundation (project - „Doctoral School of Energy and Geotechnology II“).

References

1. Akagi, H.: Trends in active power line conditioners. IEEE Trans. Power Electron. 9(3), 271–350 (1994)
2. Akagi, H.: Modern Active Filters and traditional passive filters. Bulletin of the Polish Academy of Sciences, Technical Sciences 54(3), 255–269 (2006)
3. Cadaval, E.R., Gonzalez, F.B., Montero, M.I.M.: Active power line conditioner based on two parallel converters topology. In: Compatibility in Power Electronics, pp. 134–140. IEEE (June 1, 2005)
4. Dixon, J.W., Moran, L., Elgueta, C.: Some improvements in 81-Level Inverters for Traction Applications. In: Proc. of 21th Electric Vehicle Sysmposium (EVS 21), Montecarlo, Monaco (2005)
5. Bhattacharya, S., Cheng, P.-T., Divan, D.M.: Hybrid solutions for improving passive filter performance in high power application. IEEE Trans. Industry Applications 33(3), 732–747 (1997)
6. Husev, O., Ivanets, S., Vinnikov, D.: Neuro-fuzzy Control System for Active Filter with Load Adaptation. In: Compatibility and Power Electronics CPE 2011, pp. 28–33. IEEE (2011)
7. Strzelecki, R., Benysek, G., Jarnut, M.: Power Quality Converters with Minimum Number of Current Sensor Requirement. International School on Nonsinusoidal Currents and Compensation, 1–4 (2008)
8. Ivanets, S., Husev, O., Chub, A.: Method of choice elements of active line conditioner. Journal of Chernigov State Technological University (40), 223–232 (2009)